

Mapping damages in concretes using an extended digital image correlation technique

H Mamand and J Chen*

Abstract—This paper presented an extended digital image correlation technique (EDIC) for mapping damages in concretes. A digital image camera was used to scan the surfaces of investigated concrete beams during the loading process. The developed EDIC technique was used to computationally detect macro and micro cracks, and predict micro crack propagation before the crack become visually detectable. This developed EDIC technique is essential to carry out an in-situ mapping damages in concrete structures. This new technique firstly extended the capability of current digital image correlation technique by computational detecting multiscale cracks, which enables a non-destructive test of structural damages. This developed EDIC technique can be used for further research on material damages in the society of concrete academia and applications in detecting damages of ageing concrete structures in concrete related industries.

Keywords—Extended digital image correlation, Mapping damages in concretes, Distance transformation algorithm, Critical damage strain, Multiscale crack

I. Introduction

Non-destructive test (NDT) plays an important role in damage assessment of ageing concrete structures, and in planning repairing work. Comprehensive damage assessment requires detecting macro and micro cracks. Current digital image correlation (DIC) approach, one of popular NDT techniques, can only detect macro cracks by recording images in measurement process. The objective in this study is developing an extended digital image correlation (EDIC) technique to detect macro and micro cracks developed on the beam surface, and to predict micro crack propagation for the assessment of damage levels and planning reparation.

II. Methodology

The methodology used in this investigation is computational detecting damages through the developed EDIC technique together with comparison of scanned images to determine critical damage strains then conduct computational detecting multiscale cracks in investigated concretes. The calculation of correlation can be involved in comparison and determination. The critical damage strains play an important role in detecting the multiscale cracks in concretes. The critical damage strain is the value at which crack will initiate and propagate. This will help to identify and monitor a damage zone in concretes, which is required in assessing the damage level of ageing concretes.

H Mamand and J Chen*
School of Civil Engineering and Surveying, University of Portsmouth

III. Experimental work

A number of concrete beam samples with two sizes of, 100 x 100 x 500 mm and 100 x 100 x 250 mm, dimensions were tested in laboratory. A standard DIC camera measurement system (Imager E-Lite 5M Camera – Lavisision Product) was used to monitor the deformation and failure of concrete beams subjected to gradual increment in flexural loading. Figure 1 shows a failed concrete beam at the end of the test. The test process was monitored by a DIC camera system which provides vital data of the surface damage mechanism of the tested beams, including recorded deformed and undeformed images of concrete beams. Images were recorded according to the setup of the frequency for taking images. The number of images stored was given according to the order of taking image in loading process. These data were sorted in the corresponding image correlation system for producing required information such as deformation and strains around the area of interest which was set using a rectangular boundary before the analysis begun.

IV. Digital Image Correlation

The functional relationship between the point before and after deformation as shown in Equation 1.

$$\begin{aligned} xp^* &= xp + u(x, y) \\ yp^* &= yp + v(x, y) \end{aligned} \quad (1)$$

Where, (xp, yp) and (xp^*, yp^*) are the coordinates of point P before and after deformation; $u(x, y)$ and $v(x, y)$ are the displacement functions in x and y direction respectively, calculated using the incremental coordinates. The degree of matching between subsets of pixels is quantified by the correlation coefficient (COF) shown in Equation 2.

$$COF = \left[\sum F(x, y)G(\bar{x}, \bar{y}) \right] \div \sqrt{\sum F(x, y)^2 G(\bar{x}, \bar{y})^2} \quad (2)$$

Where, $F(x, y)$ and $G(\bar{x}, \bar{y})$ are the grayscale of the undeformed sub-image on coordinate (x, y) and deformed sub-image on coordinate (\bar{x}, \bar{y}) respectively. The strain field can be computed individually using Equation 3 in which, u_{t1} , v_{t1} and u_{t2} , v_{t2} are the displacements in x and y direction of the selected points at time t_1 and time t_2 respectively. The different time point was actually taken from different images recorded in loading process in this investigation.

$$\left\{ \begin{array}{l} \varepsilon_{xx} = \frac{du}{dx} = \frac{u_{i2} - u_{i1}}{\Delta x_{i1}} \\ \varepsilon_{yy} = \frac{dv}{dy} = \frac{v_{i2} - v_{i1}}{\Delta y_{i1}} \\ \varepsilon_{xy} = \frac{du}{dy} + \frac{dv}{dx} = \frac{u_{i2} - u_{i1}}{\Delta y_{i1}} + \frac{v_{i2} - v_{i1}}{\Delta x_{i1}} \end{array} \right. \quad (3)$$

The formulas to calculate the maximum principal strain and the principal strain angle are given by the following Equations.

$$\varepsilon_{\max} = \frac{\varepsilon_{xx} + \varepsilon_{yy}}{2} + \sqrt{\frac{(\varepsilon_{xx} - \varepsilon_{yy})^2}{4}} + \varepsilon_{xy} \quad (4)$$

$$\tan 2\theta_p = \frac{\varepsilon_{xy}}{\varepsilon_{xx} - \varepsilon_{yy}} \quad (5)$$

Where, ε_{xx} and ε_{yy} are the normal strain in x and y axes respectively, ε_{xy} is the shear strain and θ_p is the principal strain angle.

V. Extended digital image correlation

The strain filed produced by DIC can be written into a matrix with $m \times n$ dimension shown in Equation 8.

$$\varepsilon_{ij} = \begin{bmatrix} \varepsilon_{11} & \varepsilon_{12} & \cdots & \varepsilon_{1n} \\ \varepsilon_{21} & \varepsilon_{22} & \cdots & \varepsilon_{2n} \\ \vdots & \vdots & \ddots & \vdots \\ \varepsilon_{m1} & \varepsilon_{m2} & \cdots & \varepsilon_{mn} \end{bmatrix} \quad (8)$$

The developed EDIC used a created mathematical function, distance transform algorithm (DTA) together with the function of maximum stationary point (MSP) to compute the distance transform for plotting a crack path along the dominated damage track of the damaged zone. This dominated damage track was recognised as a crack path in which every point has an equal distance to the side edges of the damaged zone.

In NDT calculation, the sing result, $slope(\varepsilon_{ij})$ between two points can be calculated by Equation 9.

$$slope(\varepsilon_{ij}) = sign(diff(\varepsilon_{ij} - \varepsilon_{i(j-1)})) \quad (9)$$

The sign function is a mathematical expression defined by the Equation 10.

$$sign(\varepsilon_{ij}) = \begin{cases} -1 & \text{if } \varepsilon_{ij} - \varepsilon_{i(j-1)} < 0 \\ 0 & \text{if } \varepsilon_{ij} - \varepsilon_{i(j-1)} = 0 \\ 1 & \text{if } \varepsilon_{ij} - \varepsilon_{i(j-1)} > 0 \end{cases} \quad (10)$$

The local peak value at each row of strain matrix is identified by the Equation 11.

$$\left\{ \begin{array}{l} slope(\varepsilon_{ij}) = 1, slope(\varepsilon_{ij}) \in R \\ peak(\varepsilon_{ij}) | slope(\varepsilon_{ij}) + slope(\varepsilon_{i(j+1)}) = 0 \end{array} \right. \quad (11)$$

Where, the R is an array of sign results in potential damage region. Finally, all peak values obtained from each row of strain matrix in damage region were sent into an array P given by Equation 12 to plot crack paths.

$$P = \sum_{i=1}^n peak(\varepsilon_i) \quad (12)$$

Equations 1 to 12 were used in the development of EDIC based programme. This programme was developed by Matlab. This EDIC programme was used in this investigation to computationally detect failed patterns with macro and micro cracks in the following three concrete samples tested in a structural laboratory.

VI. Results and comparison

Figure 2a shows two of recorded images of failed concrete samples with cracks during the loading process. Figure 2b displays the deformed meshes by recorded images at the failure points given by current DIC camera system. It can be seen from Figure 2b that current DIC camera system can only present the deformed meshes except recorded images. However, the developed EDIC technique can conduct a crack path along the dominated damage track in the damaged zone. This can be seen from Figure 2c in which the width of crack dictates the amount of strain scaled by the local peak values of principal strains at each row of strain matrix in the damaged area. The direction of crack growth at each point given in Figure 2c was associated with the principal strain vectors.

Figure 3 shows tested results of another sample recorded at the images 475 and 480 together with the EDIC detection of multiscalar cracks. It is hardly to say a visible crack shown in Figure 3a at the early image 475. As the loading level increased, a macro crack was clearly recorded at the image 480 shown in Figure 3c. Actually, this macro crack has been detected by the EDIC as a micro crack at the corresponding loading level of image 475 shown in Figure 3b. Therefore, the macro crack appeared at the later images can be detected as a micro crack by the EDIC at the earlier image or lower loading level, which are undetectable by current DIC camera system.

References

- [1] *The Relevance of Microcracking* 2009 Retrieved from the Concrete Construction website <http://www.concreteconstruction.net/internet/the-relevance-of-microcracking.aspx>
- [2] Kiani K and Shodja H M 2011 Prediction of the penetrated rust into the microcracks of concrete caused by reinforcement corrosion *Applied Mathematical Modelling* **35** 2529-2543
- [3] Jacobsen J S, Poulsen P N, Olesen J F and Krabbenhoft K 2013 Constitutive mixed mode model for cracks in concrete *Engineering Fracture Mechanics* **99** 30-47
- [4] Davis L S 2011 User Manual 8
- [5] Robertson M A, Borman S and Stevenson R L 1999 Dynamic range improvement through multiple exposures *Image Processing 1999 ICIP 99 Proc. IEEE* **3** 159-163
- [6] Lecompte D, Vantomme J and Sol H 2006 Crack detection in a concrete beam using two different camera techniques *Structural Health Monitoring* **5** 59-68
- [7] Sutton M A, Ortu J J and Schreier H W 2009 Image correlation for shape, motion and deformation measurements *Springer US* **10** 978-0
- [8] Tung S H and Sui C H 2010 Application of digital image correlation techniques in analysing cracked cylindrical pipes *Sadhana* **35** 557-567
- [9] Mathworks 2014 Image Processing Toolbox: User's Guide (R2014a)
- [10] Vrech S M and Etse G 2012 Discontinuous bifurcation analysis in fracture energy based gradient plasticity for concrete *International Journal of Solids and Structures* **49** 1294-1303
- [11] Wu S, Chen X and Zhou J 2012 Tensile strength of concrete under static and intermediate strain rates: Correlated results from different testing methods *Nuclear Engineering and Design* **250** 173-183
- [12] Mosley B, Bungey J and Hulse R 2007 *Reinforced concrete design to Eurocode 2* 6th edn (Basingstoke: Palgrave Macmillan)
- [13] Lu Y B and Li Q M 2011 About the dynamic uniaxial tensile strength of concrete-like materials *International Journal of Impact Engineering* **38** 171-180
- [14] Ortiz M 1987 An analytical study of the localized failure modes of concrete *Mechanics of Materials* **6** 159-174
- [15] M. Young, *The Technical Writer's Handbook*. Mill Valley, CA: University Science, 1989.

About Author (s):



Dr Jiye Chen, Senior Lecturer, School of Civil Engineering and Surveying, University of Portsmouth, UK. Research interests include: Computational damage mechanics of fibre composites, Non-destructive test technique, Multiscale modelling technique, Design, Analysis and Test of Composite Structures, etc.

Figure 4 presents that the EDIC detected multiscale cracks together with images recorded at varied loading levels. It should be noticed that the increased loading levels are equivalent to the continually recorded image numbers in experimental work. It can be seen from Figure 4a that the image 447 shows a visible or macro crack at the lower part of beam. Figure 4b shows a micro crack marked by a red circle detected by the EDIC at the corresponding loading level of the image 447. Obviously, this micro crack was not caught by DIC camera at the image 447. As loading increased, the image 448 presented a further visible or macro crack shown in Figure 4c. Through comparing Figures 4b and 4c, the macro crack given by the image 448 proved the EDIC computational detection of a micro crack at the image 447 shown in Figure 4b. It should be noticed that a critical damage strain of 0.02 was used in the computational detecting a micro crack in this investigation.

VII. Conclusion and future work

The developed EDIC technique was successfully used in computational detecting multiscale cracks in concrete beams under bending. The EDIC played an important role in detecting the damaged area with macro and micro cracks. The full damage models of tested concrete beams were achieved by the developed EDIC technique with a distance transformation algorithm. Applications in this investigation have shown that the EDIC technique is able to detect multiscale cracks. This advantage can essentially help the determination of the damaged area of concretes which needs assessment and repair. This developed EDIC technique has potential to carry out a practical measurement on site to provide a comprehensive damage level of the ageing concrete structures, to detect further crack propagation for ensuring a safe usage of the ageing concrete structures and planning repair.

The developed technique EDIC can also be applied into reinforced concretes for safety assessment in the future. The currently developed EDIC technique as a 2D system can only be used for detecting multiscale cracks on the flat surface of objects. The future work will consider extending the developed technique EDIC from a 2D system to a 3D system for mapping damages of the objects with curved surfaces. Future work will also include further validation of the EDIC on computational detecting the micro crack propagation through more applications.

Acknowledgment

The authors would like to acknowledge the UK BAE systems surface ships limited for their granting this research and permission to publish this article.



Fig. 1. A failed concrete beam sample

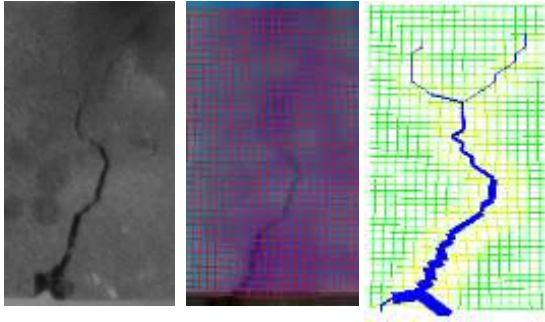


Fig. 2. a. Image with cracks b. Meshed image
c. Macro and micro crack paths

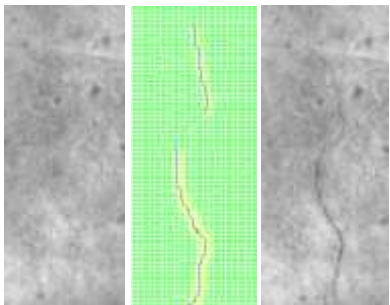


Fig. 3. a. The image 475 with no visible crack; b. The EDIC detected micro cracks at the image 475 which is not shown in a; c. A further image 480 with a crack growth proving the micro crack shown in b

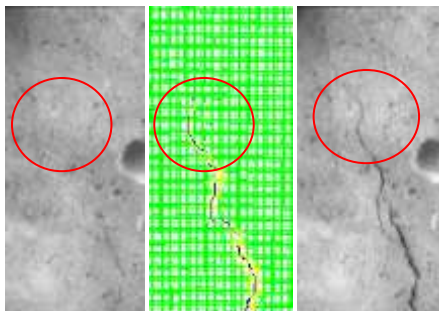


Fig. 4. a. The image 447 with a macro crack; b. The EDIC detected micro crack marked by a red circle which is not shown in a; c. A further image 448 with a crack growth proving the micro crack shown in b.